

Received May 20, 2019, accepted June 13, 2019, date of publication June 19, 2019, date of current version July 15, 2019.

Digital Object Identifier 10.1109/ACCESS.2019.2923767

# Queue-Aware Cell Activation and User Association for Traffic Offloading via Dual-Connectivity

QIAONI HAN<sup>1</sup>, BO YANG<sup>2,3</sup>, (Senior Member, IEEE), AND XIAOCHENG WANG<sup>4</sup>

<sup>1</sup>School of Electrical and Information Engineering, Tianjin University, Tianjin 300072, China

<sup>2</sup>Department of Automation, Shanghai Jiao Tong University, Shanghai 200240, China

<sup>3</sup>Key Laboratory of System Control and Information Processing, Ministry of Education of China, Shanghai Jiao Tong University, Shanghai 200240, China

<sup>4</sup>Department of Electronics, Shanghai Jiao Tong University, Shanghai 200240, China

Corresponding author: Qiaoni Han (qnhan@tju.edu.cn)

This work was supported in part by the National Natural Science Foundation of China under Grant 61803218, Grant 61731012, and Grant 61573245, in part by the Natural Science Foundation of Shandong Province of China under Grant ZR2019BF005, and in part by the Key R&D Project of China under Grant 2016YFB0901900 and Grant 2018YFB1702300.

**ABSTRACT** With the objective of reducing energy cost, we study the stochastic optimization of traffic off-loading via dual-connectivity by joint cell activation and user association. Particularly, explicitly considering the dynamic effects of time-varying and random traffic arrivals, we formulate a stochastic problem that quantifies the tradeoff between energy cost and queuing delay. Employing two-time-scale Lyapunov optimization, the formulated problem is transformed as a user association problem at each time slot and a small-cell activation problem at each frame. However, the user association problem turns out to be a mixed-integer nonlinear programming problem and is difficult to be transformed into a convex problem, and traditional game-theoretic solutions, such as Nash equilibrium, cannot be used to solve it. Then, we introduce a two-sided many-to-one matching game and propose a distributed user association algorithm that converges to a local optimum. On the other hand, the cell activation problem belongs to the class of maximum facility location problems that are generally NP-hard. Additionally, its objective function is not a submodular one. Thus, we present an iterative and heuristic algorithm that finds the best set of active small-cell BSs by repeatedly solving the user association problem with different sets of active small cells in each iteration. Furthermore, an online two-time-scale joint cell activation and user association algorithm are developed. Finally, numerical results show the effectiveness of the matching-based user association algorithm on traffic off-loading improvement, the heuristic cell activation algorithm on trading off between energy cost reduction and network throughput enhancement, and the online joint algorithm on balancing between energy cost reduction and queuing delay performance.

**INDEX TERMS** Small cell dual-connectivity, cell activation, user association, two-time-scale Lyapunov optimization.

## I. INTRODUCTION

The explosive growth of global mobile data traffic and the increasing environment and economic concerns have led to a more urgent requirement for both area spectral efficiency and energy efficiency [1]. In this context, the wireless infrastructure has evolved to an increasingly dense and heterogeneous architecture, where various access points (APs) with

different radio access technologies (RATs), coverage areas and backhaul capabilities are deployed and operate in disparate frequency bands and bandwidths. As a result, most of the mobile users in such a dense wireless network would be likely to lie in the overlapping coverage areas of multiple RATs, which motivates the traffic offloading of macrocell through optimally leveraging such simultaneous availability of multiple RATs. Further, the architectures above are being standardized as distributing traffic across cellular (LTE) and wireless LAN (WLAN) through LTE-WLAN

The associate editor coordinating the review of this manuscript and approving it for publication was Cunhua Pan.

Aggregation (LWA) [2], [3] and traffic splitting across an anchor (macrocell) and a booster (small cell), i.e., dual-connectivity (DC) [4]–[7]. Particularly, DC is gaining attention from both 3GPP LTE-A standardizing activities and industry practice [8], [9], and the focus for DC in *Rel-12* was mostly on the downlink throughput enhancements, while new *Work Items* were proposed in *Rel-13* to 15 and beyond to continue with the further development of DC [10].

Through effectively exploiting the additional network capacities provided by multi-tiered small cells, DC achieves flexible traffic schedule, efficient traffic offloading and low-cost network infrastructure upgrade. Given the fact that more and more user devices are equipped with multiple radio-interfaces, traffic offloading via DC becomes increasingly attractive [5], [11], [12]. However, when it comes to the techniques to realize these gains enabled by DC, recent works were based on static models without involving the dynamic and stochastic features into problem formulation. Further, none of those works gave consideration to energy saving while energy-efficiency is one of the major design goals for wireless cellular networks [1].

On the other hand, since high energy consumption in radio access networks accounts for a significant proportion of the operational expenditure of operators [13], the operators have incentives to reduce energy consumption through novel hardware design, efficient resource management and dynamic BS activations [14]–[16]. Generally, transmission power control is a common method. But, considering various sources of energy consumption in the BS equipment, such as cooling system and processing unit, transmission power control alone cannot be effective enough. Particularly, with current BSs, even in idle or low traffic state, about 50 – 90% of peak energy (energy consumed during peak traffic) is consumed and appropriately turning off some BSs is preferably [17]. In addition, there is a fundamental tradeoff between energy consumption and queuing delay [18], thus it is important to balance their tradeoff so as to reduce energy cost while satisfying QoS requirement.

In this work, we focus on the energy cost minimization-oriented traffic offloading problem through proper small cell activation and user association (i.e., small cell selection) in the case of DC, where users are served by both macrocell and one small cell (picocell, femtocell or Wi-Fi) with the following considerations: First, we assume that all the backhaul links between small cell BSs and the macro-BS are ideal, thus DC is easy to be implemented. Second, since a small cell BS consumes less energy than the macro-BS, the operator of an integrated macrocell and small cell network can reduce overall energy consumption by offloading parts of cellular traffic to small cells. Third, for energy saving of network and QoS guarantee of mobile users, switching off some small cell BSs is more easily to be operated and has smaller effects on the service provision quality. At last, the cell activation and user association decisions should be adaptive to time-varying and random traffic arrivals.

To sum up, there are three major challenges in our concerned optimization problem. Firstly, we consider a stochastic system where both traffic arrivals and channel conditions of users change over time, which require an online algorithm that dynamically selects appropriate small cells as the boosters of users for traffic offloading and switches off unnecessary small cell BSs for energy saving based on non-causal information at hand. Secondly, the user association is performed much more frequently than the cell activation, which requires the determination of cell activation and user association in two time scales. Moreover, the actions of user association and cell activation are tightly coupled that affect the total energy cost. Thirdly, to reduce the total energy cost while providing delay guarantee to all users, a good balance should be kept by jointly optimizing cell activation and user association. Since a long period of time is considered, the cell activation and user association decisions are strongly correlated in both spatial and temporal domains. Overall, distinguished from the static optimization problems recently studied, the problem considered in this paper is formulated as a stochastic optimization in two time scales.

In a nutshell, the contributions of this work are:

- 1) Considering time-varying and random traffic arrivals for energy cost minimization-oriented traffic offloading via DC, we formulate a stochastic optimization for joint cell activation and user association.
- 2) Leveraging on two-time-scale Lyapunov optimization approach, we develop an online queue-aware joint algorithm for energy cost minimization by choosing the active set of small cell BSs and determining the association of users based on queue and channel state information in the large- and small-time-scale respectively. In this way, without relying on any statistic knowledge of the system, the traffic demands of all the users are satisfied while incurring minimum energy cost.
- 3) The delay and energy cost performance of the proposed algorithm is evaluated by numerical results. Due to its adaptive to queue state information, the proposed algorithm achieves significant performance gain and can provide a flexible and efficient means to control the tradeoff between energy cost and delay.

The rest of the paper is organized as follows. Section II summarizes the recent study on traffic offloading via DC and tradeoff between energy cost and QoS performance. The system model and problem formulation are given in Section III. Section IV details the online joint cell activation and user association algorithm. Section V presents the performance evaluation. Finally, Section VI concludes the paper.

## II. RELATED WORK

### A. TRAFFIC OFFLOADING VIA DC

In regards to the techniques to realize traffic offloading gains enabled by DC, the detailed system-level simulations to show that how DC can improve end-user throughput and mobility performance were given in [5]; [19] proposed the concept

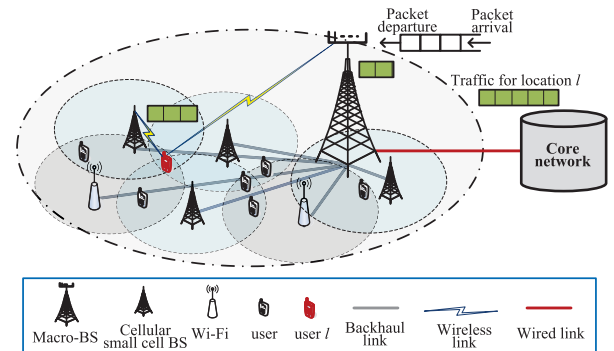
**TABLE 1.** Comparisons between this work and reference [27]–[29].

	Network scenario	Focused issue
This work	time-varying, heterogeneous networks with DC	joint cell activation and user association
[27]	static, an infrastructure-based wireless network	joint BS operation and user association
[28]	time-varying, homogeneous cellular networks	BS activation
[29]	time-varying, C-RAN	joint RRH activation and beamforming

of flexible cell association in DC scenarios and derived the DC association regions for decoupled access; [20] developed a flow control algorithm where the macro-BS and small cell BSs are interconnected with traditional backhaul links; considering non-ideal backhaul links, Singh S. *et al.* proposed an optimal traffic aggregation solution accounting for backhaul delay [21]; while Wu Y. *et al.* jointly determined each mobile user's traffic schedule (between macro-BS and small cell AP) and power control (between two radio-interfaces) for uplink transmission in [22], and jointly optimized the BS's bandwidth allocation as well as the mobile user's traffic scheduling and power allocation in [23]. Moreover, there are works focusing on the general "multi-homing" scenario. Among them, [24] proposed a multi-RAT interface activation algorithm; [25] solved a joint user assignment and data rate allocation problem to maximize total utility; and the outage probability and spectral efficiency associated with different degrees of multi-connectivity in a typical 5G urban scenario were characterized in [26]. In contrast, we take into consideration the dynamic and stochastic features into the problem formulation and put energy saving as one of the system design objectives.

### B. TRADEOFF BETWEEN ENERGY COST AND QoS PERFORMANCE

Since it is important to balance the tradeoff so as to reduce energy cost and satisfy QoS requirement at the same time, recently, [27], [28] and [29] have jointly considered these two aspects under different scenarios. Based on a static model of an infrastructure-based wireless network with multiple BSs, [27] formulated a total cost minimization problem allowing a flexible tradeoff between flow-level performance and energy consumption; giving a general cellular networks with homogeneous BSs, an online control algorithm to choose active set of BSs so as to satisfy users' demands while incurring minimum energy consumption was developed in [28], where user association issue was omitted due to the homogeneity of BSs; considering a downlink slotted cloud radio access network (C-RAN), [29] proposed a joint radio remote head (RRH) activation and beamforming algorithm accounting for random traffic arrivals and time-varying channel fading. While differing from these works in network scenario and focused issue, we solve an energy cost minimization problem for heterogeneous networks with DC by designing a joint cell activation and user association algorithm, where the interactional small cell activation and user association in two time scales are adaptive to time-varying and random traffic arrivals. For clarity, the

**FIGURE 1.** An example of the considered network model.

comparisons between this work and [27]–[29] are summarized in Table.1.

## III. SYSTEM MODEL AND PROBLEM FORMULATION

### A. NETWORK MODEL

We consider the downlink transmission in a slotted system and focus on the monopoly case, where a single operator provides coverage for a geographic area by its own macro-BS with massive MIMO and small cell BSs. Here, "small cell BS" is a generic term to represent cellular pico-BSs, femto-BSs, and Wi-Fi APs collectively. To facilitate the implementation of DC, we assume that

- 1) The macro-BS serves as the gateway (system controller) and provides ideal backhaul for all the small cell BSs.
- 2) All the users have the capability of aggregating traffic from both the macrocell and small cells.
- 3) The small cell BSs operate on a different frequency from that of the macrocell, and cellular pico- and femto-BSs reuse the same frequency.
- 4) The split of traffic occurs at the macro-BS, and all the BSs are tightly synchronized.
- 5) The macro-BS assists the user association determination and executes the small cell activation algorithm.

Fig. 1 gives the considered network model. For clarity, the set of small cell BSs is denoted by  $\mathcal{N} = \{1, \dots, N\}$ , where the sets of Wi-Fi APs and cellular small cell BSs are respectively  $\mathcal{N}_1$  and  $\mathcal{N}_2$ ,  $\mathcal{N}_1 \cup \mathcal{N}_2 = \mathcal{N}$ ,  $\mathcal{N}_1 \cap \mathcal{N}_2 = \emptyset$ . All the small cell BSs offload the macro-BS by jointly providing coverage for the set  $\mathcal{L} = \{1, \dots, L\}$  of locations, where multiple users can be presented in a single location.<sup>1</sup>

<sup>1</sup>Given the fact that availabilities of Wi-Fi networks are location-dependent [30], we consider locations instead of individual users. Moreover, such a network model is consistent with heterogeneous cellular networks based on LTE technology [28]

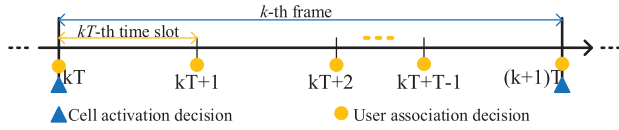


FIGURE 2. An illustration of two-time-scale operations.

To reduce energy consumption, when the data traffic is small, the system controller can turn off some small cell BSs. Further, to avoid unnecessary overhead (e.g., energy consumption, QoS degradation, delays) caused by frequent on/off switch, BS activation and deactivate should be carried out at a time scale that is larger than other normal operations such as user association. Therefore, here, we divide the overall time into frames of size  $T$  time slots, and assume that:

- 1) The activate and deactivate decisions of small cells are made at the beginning of each frame (large-time-scale);
- 2) The association of locations with small cells is determined at the beginning of every time slot (small-time-scale).

Such a two-time-scale structure is illustrated in Fig. 2.

Further, we introduce a binary set  $\mathcal{Y}(t) = [y_n(t)]_{|\mathcal{N}_1|}$  with

$$y_n(t) = \begin{cases} 1, & \text{if small cell BS } n \text{ is active at time slot } t, \\ 0, & \text{otherwise.} \end{cases} \quad (1)$$

to denote the state set of small cell BSs at time slot  $t$ .

## B. RATE MODEL

Denoting by  $r_{l,n}$  the throughput or long-term rate achieved by a location  $l$  from a cell  $n$ , which depends on the RAT of cell  $n$ , the location-specific parameters and the other locations that associated with cell  $n$ . While the instantaneous physical rate  $R_{l,n}(t)$  of location  $l$  from cell  $n$  depends on its selected modulation and coding scheme and the average channel conditions between location  $l$  and cell  $n$  at time slot  $t$ , owing to the fact the user association is carried out in a large time scale compared with the change of channels. Moreover, the different access networks in heterogeneous networks have different medium access (MAC) protocols to share the radio resources among users. Referring to [31], the MAC protocols are divided into two classes, and for a Wi-Fi AP  $n \in \mathcal{N}_1$ , the long-term downlink rate of a location  $l$  served by it depends on the specific locations that are connected to it and can be expressed as

$$r_{l,n} = \frac{S}{\sum_{i \in \mathcal{L}^{x_{i,n}}} S / R_{i,n}}, \quad 0 \leq r_{l,n} \leq r_{n,max}^W, \quad (2)$$

where the binary variable  $x_{i,n}$  is defined as

$$x_{i,n} = \begin{cases} 1, & \text{if location } i \text{ is served by small cell BS } n, \\ 0, & \text{otherwise.} \end{cases} \quad (3)$$

$S$  is the fixed packet size, and we adopt the general function of  $R_{i,n}$  defined in [32], i.e.,  $R_n = \frac{P_{tr} P_s G}{(1-P_{tr})T_b + P_{tr} P_s T_s + P_{tr}(1-P_s)T_c}$ ,

where  $G$  is the average payload length,  $T_b$  is the back-off slot size,  $T_s$  and  $T_c$  are respectively successful transmission slot size and collision slot size,  $P_{tr} = 1 - (1 - \phi)^{L_n}$ ,  $P_s = \frac{L_n \phi (1 - \phi)^{L_n - 1}}{1 - (1 - \phi)^{L_n}}$  with  $\phi$  being the transmission probability and  $L_n = \sum_{l \in \mathcal{L}^{x_{l,n}}} 1$  being the number of locations associated with Wi-Fi AP  $n$ . Besides, according to (2), all the locations served by the same Wi-Fi AP achieve equal long-term rate. Actually, this is due to the fact that a Wi-Fi AP provides fair access opportunity to its associated locations. The long-term rate of the locations on the downlink depends on the queuing technique implemented on the Wi-Fi AP. By adopting the most common technique, i.e., the round-robin scheme, all the locations that share the same Wi-Fi AP achieve the same downlink long-term rate.

While the long-term downlink rate of a location  $l$  served by the LTE macrocell and small cell (picocell, femtocell) with resource-fair MAC protocol can be respectively expressed as

$$r_{l,0} = R_{l,0}/L_0, \quad \forall l \in \mathcal{L}_0 \quad (4)$$

$$0 \leq r_{l,n} = R_{l,n}/L_n \leq r_{max}, \quad \forall l \in \mathcal{L}_n \quad (5)$$

where  $L_0 = L$  and  $L_n = \sum_{l \in \mathcal{L}^{x_{l,n}}} 1$  are the number of locations sharing macro-BS and cellular small cell BS  $n \in \mathcal{N}_2$ , respectively, and  $\mathcal{L}_0$  and  $\mathcal{L}_n$  are their sets. For locations served by the macro-BS with massive MIMO, by referring to the results in [33] and borrowing results for the well-known case of Zero-Forcing Beamforming precoding and *i.i.d.* (independent and identically distributed) Rayleigh fading, the instantaneous rate in (4) can be approximated with a simple, accurate rate  $R_{l,0} = F_0 W_0 \log_2 \left( 1 + \frac{M_0 - F_0 + 1}{F_0} \frac{P_0 h_{l,0}}{\sigma_0^2} \right)$ , where  $W_0$  and  $M_0$  are the bandwidth and the number of antennas of the macro-BS, respectively and  $F_0$  is the prefixed load parameter of the macro-BS indicating how many locations it could serve (it is noted that the sum activities of all the locations being served by macro-BS cannot exceed the beamforming subset size  $F_0$ , i.e.,  $L \leq F_0$ ),  $P_0$  is the transmission power of the macro-BS,  $\sigma_0^2$  is the noise power level,  $h_{l,0}$  denotes the large-scale fading channel power gain between macro-BS and location  $l$ , and there is no small scale fading factor in  $R_{l,0}$ . Moreover,  $R_{l,n} = W \log_2 \left( 1 + \frac{P_n^C g_{l,n}}{\sigma_n^2 + \sum_{j \neq n, j \in \mathcal{N}_2} P_j^C g_{l,j}} \right)$ , where  $W$  is the shared bandwidth of cellular small cells,  $\sigma_n^2$  denotes the noise power level,  $g_{l,n}$  is the average channel power gain (i.e., the large-scale slow-fading) between cellular small cell BS  $n$  and location  $l$ , owing to the larger time scale of user association compared to that of channel varying [34].

*Remark 1:* It is noted that the transmission power of the macro-BS and an active small cell BS is assumed to be fixed in the above rate model. Obviously, the optimal power allocation of the BSs will do help reduce the energy cost but complicate the problem to be solved. In the future, we will work on the joint cell activation, user association and power allocation for energy cost minimization in heterogeneous works with DC.

**C. TRAFFIC MODEL**

The traffic intended for location  $l \in \mathcal{L}$  is first received at the gateway (macro-BS) and stored in the queues  $Q_l(t)$ .<sup>2</sup> The traffic arrivals (bits) at time slot  $t$  are denoted by  $A(t) = [A_1(t), \dots, A_L(t)]$ , and we assume  $A_l(t)$  is *i.i.d.* over the whole frame and follows a general distribution with mean  $\bar{A}_l$  was known to the gateway [28]. In addition, we assume  $A_{min} \leq A_l(t) \leq A_{max}, \forall l \in \mathcal{L}$ .

Since DC is adopted, the data stored in queue  $Q_l(t)$  will be distributed between the macro-BS and one small cell BS that provides service to location  $l$ . Specifically, the traffic at location  $l$  is routed to the macro-BS and one small cell BS  $n$  with amount  $\mu_{l,0}(t)$  and  $\mu_{l,n}(t)$ , respectively, at time slot  $t$ , and  $\mu_{l,0}(t) = \Delta t r_{l,0}(t)$ ,  $\mu_{l,n}(t) = \Delta t x_{l,n}(t) y_n(t) r_{l,n}(t)$ , where  $\Delta t = 1$  is the time duration of time slot  $t$ .

Moreover, the assumption that the macro-BS keeps buffers for the data that is not transmitted yet simplifies the considered queuing model. Since the decisions are made based on the whole backlog of each location, this assumption will not affect the solution. In addition, we assume that the total rate provided for each location is upper bounded by  $\mu_{max}$ , i.e., the inequality  $0 \leq \mu_{l,0}(t) + \sum_{n \in \mathcal{N}} \mu_{l,n}(t) = \sum_{n \in \mathcal{N}} \mu_{l,n}^s(t) \leq \mu_{max}$  holds for each location  $l \in \mathcal{L}$ . In this context, the evolution of queues in consecutive time slots are expressed as,

$$Q_l(t+1) = [Q_l(t) - \sum_{n \in \mathcal{N}} \mu_{l,n}^s(t)]^+ + A_l(t), \quad \forall l \in \mathcal{L}, \quad (6)$$

where  $[x]^+ = \max\{x, 0\}$ , and the system is said to stable if the following conditions on queue backlogs hold,

$$\limsup_{t \rightarrow \infty} \frac{1}{t} \sum_{\tau=0}^{t-1} \mathbb{E}\{Q_l(\tau)\} < \infty, \quad \forall l \in \mathcal{L}. \quad (7)$$

**D. POWER MODEL**

Referring to [35], the power consumption  $P_n^{W,ov}$  of Wi-Fi AP  $n \in \mathcal{N}_1$  can be expressed as follows:

$$P_n^{W,ov} = \begin{cases} P_n^{W,a}(L_n) = \frac{(1-P_{tr})E_b + P_{tr}P_sE_s + \sum_{j=2}^{L_n} P_{c,j}E_{c,j}(L_n)}{(1-P_{tr})T_b + P_{tr}P_sT_s + P_{tr}(1-P_s)T_c} \\ P_n^{W,s}, \text{ if } y_n = 0 \end{cases} \quad (8)$$

where  $P_{c,j} = \binom{L_n}{j} \phi^j (1-\phi)^{L_n-j}$  and  $E_b$ ,  $E_s$ , and  $E_{c,j}(L_n)$  are the energy consumption of the backoff slot, successful transmission, and  $j$  collided transmissions, respectively, and  $P_n^{W,a}$  and  $P_n^{W,s}$  are respectively the power consumption of the active and sleep Wi-Fi AP  $n$ . In [36], the approximate power consumption models of cellular small cell BSs are established, where a radio frequency (RF) chain refers to a set of hardware components composed of a small-signal transceiver section,

<sup>2</sup>Our model only needs the backlog state information of each location, while in practice, queues might reside in serving BSs and their size information is fed back to the gateway.

a power amplifier (PA) and the antenna interface. Among them, PA consumes a large share of overall power due to its low efficiency, and RF chains can be switched off or put into sleep mode individually when there is no transmission on the respective antenna. According to this model, the relationship between RF output power  $P_n^C$  and overall BS power consumption  $P_n^{C,ov}$  is given by:

$$P_n^{C,ov} = \begin{cases} P_n^{C,a} = P_n^0 + \Delta_n P_n^C, & \text{if } 0 \leq P_n^C \leq P_{n,max} \\ P_n^{C,s}, & \text{if } P_n^C = 0 \end{cases} \quad (9)$$

where  $P_n^0$  is the power consumption calculated at the minimum possible output power, and  $\Delta_n$  is a coefficient representing the dependency of the required input power on traffic load.  $P_n^{C,a}$  and  $P_n^{C,s}$  are respectively the power consumption of an active and sleep cellular small cell BS  $n \in \mathcal{N}_2$ .

While for massive MIMO systems, since an infinite energy efficiency can be achieved as the number of antennas goes to infinity, the assumption that the power consumption of a conventional BS is proportional to the radiated transmit power is misleading. Thus, we adopt the model in [37], i.e.,

$$P_0^{ov} = P_0 / \Delta_0 + \sum_{m=0}^3 C_{m,0} S^m + \sum_{m=0}^2 C_{m,1} S^m M_0, \quad (10)$$

which clearly specifies the relationship between power consumption  $P_0^{ov}$  and antenna number  $M_0$ .  $P_0$  and  $\Delta_0$  are the transmission power and PA efficiency of the macro-BS, respectively,  $C_{m,0}$  and  $C_{m,1}$  are coefficients.

The overall power consumption of the system at time slot  $t$  is

$$P(t) = P_0^{ov} + \sum_{n \in \mathcal{N}_1} [y_n(t) P_n^{W,a} + (1 - y_n(t)) P_n^{W,s}] + \sum_{n \in \mathcal{N}_2} [y_n(t) P_n^{C,a} + (1 - y_n(t)) P_n^{C,s}]. \quad (11)$$

**E. ENERGY MODEL**

We assume that all the BSs in this geographic area are powered by one or more energy retailers, and the operator can also utilize renewable energy and finite-capacity energy storage devices to minimize the energy cost. Therefore, some energy scheduling approaches can be appropriately adopted. Here, we omit the optimization of energy scheduling, and focus on jointly optimizing cell activation and user association via DC so as to minimize the total energy cost, which is regarded to be proportional to the overall energy consumption, i.e., at time slot  $t$ , the total energy cost is denoted by.<sup>3</sup>

$$C(t) = \omega(t) P(t) \Delta t, \quad (12)$$

where  $\omega(t) > 0$  is the energy price at time slot  $t$ , and for simplicity, we assume it is fixed and  $\omega(t) \Delta t = 1$ .

<sup>3</sup>Obviously, the proposed algorithm can be applied to the case where the energy supply of all the BSs is controlled by a power supply system, and it can be easily extended to the general scenario where each BS has its own power supply system.

## F. PROBLEM FORMULATION

We aim to design an online joint small cell BS activation and user association algorithm by solving the following stochastic energy cost minimization problem:<sup>4</sup>

$$\begin{aligned} \text{P1: } \quad & \min \limsup_{t \rightarrow \infty} \frac{1}{t} \sum_{\tau=0}^{t-1} \mathbb{E}\{C(\tau)\} \\ & \text{s.t. (1), (3), (7)} \end{aligned} \quad (13)$$

where the expectation  $\mathbb{E}$  is taken with respect to the distribution of the system's energy cost, which depends on the random cell activation set and user association relation. (7) is the network stability constraint to guarantee a finite queue length for each queue.<sup>5</sup> (1) and (3) are the constraints on the state of small cell BSs and user association, respectively.

## IV. ONLINE ALGORITHM DESIGN

To know all future information on time-varying and random traffic arrivals is not practical, and current control decisions are coupled with the future ones. To deal with this, the commonly used dynamic programming suffers from a curse of dimensionality. On the other hand, it is pointed out in [18], [27]–[30], [38] that the stochastic control and delay analysis in practice is usually investigated from the queue stability perspective in a time-varying system using the Lyapunov optimization technique. In this work, given the time-varying and random traffic arrivals shown in subsection III-C and the energy cost minimization problem in subsection III-F, the formulated energy cost minimization problem by joint cell activation and user association in (13) belongs to the class of constrained optimization problems of time-varying systems, and the Lyapunov optimization framework enables the online algorithm design for such constrained optimization of time-varying systems by transforming the stochastic optimization problem into a deterministic one at each time slot. Particularly, the above cell activation and user association model fits well into the two-stage Lyapunov optimization framework. In the following, using two-time-scale Lyapunov optimization method, we detail the online control strategy design at two levels of time granularity.

### A. LYAPUNOV DRIFT FORMULATION

Firstly, the Lyapunov function  $L(t)$  is defined as a scalar measure of queue backlog as follows,

$$L(t) = \sum_{l=1}^L \frac{1}{2} [Q_l(t)]^2. \quad (14)$$

<sup>4</sup>“Online” emphasizes that the algorithm relies on limited or no future information, as opposed to an “offline” one that requires complete future information. We focus on the study of the online algorithm since it is not practical to know all future information on the system randomness.

<sup>5</sup>The queue stability constraint is used to depict and control the average delay. According to (7), queue stability is guaranteed if the average queue length is finite. Note that average delay is proportional to average queue length for a given traffic arrival rate from Little's Theorem. As proved in [38], the average queue length can be arbitrarily bounded by choosing an appropriate control parameter.

By pushing the Lyapunov function towards a lower congestion state persistently so as to keep the system stable, we introduce the  $T$ -time-slot conditional Lyapunov drift as:

$$\Delta_T(t) = \mathbb{E}\{L(t+T) - L(t) | \mathbf{Q}(t)\}. \quad (15)$$

Then following the Lyapunov drift-plus-penalty framework, we add a function of the expected operational cost over  $T$  time slots (i.e., the penalty function) to (15), and obtain the drift-plus-penalty term given as:

$$\Delta_T(t) + V \mathbb{E}\left\{ \sum_{\tau=t}^{t+T-1} C(\tau) \right\}, \quad (16)$$

where  $\mathbb{E}$  is the conditional expectation with respect to the distribution of energy cost given queue states  $\mathbf{Q}(t)$ , and  $V > 0$  is chosen to control the tradeoff between energy cost and congestion (i.e., delay, reflected in queue backlogs). A larger  $V$  means more emphasis will be put on energy cost minimization during optimization. While when  $V$  is small, network congestion carries more weight. In Lyapunov optimization, the next derivation step is to find an upper bound on this expression.

*Theorem 1 (Drift-Plus-Penalty Bound):* Let  $V > 0$  and  $t = kT$  for some  $k \in \mathbb{R}_+$ . Given any set of feasible small cell activation decision  $Y(t)$  and user association  $x(t)$ , there is,

$$\begin{aligned} \Delta_T(t) + V \mathbb{E}\left\{ \sum_{\tau=t}^{t+T-1} C(\tau) \right\} &\leq B_1 T + V \mathbb{E}\left\{ \sum_{\tau=t}^{t+T-1} C(\tau) \right\} \\ &- \mathbb{E}\left\{ \sum_{\tau=t}^{t+T-1} \sum_{l \in \mathcal{L}} Q_l(\tau) \left[ \sum_{n \in \mathcal{N}} \mu_{l,n}^s(\tau) - A_l(\tau) \right] | \mathbf{Q}(t) \right\}, \end{aligned} \quad (17)$$

where,  $B_1 = \frac{1}{2} L (A_{max}^2 + \mu_{max}^2)$ .

*Proof:* Assuming  $\tau \in [t, t+T-1]$ , through squaring the queuing dynamics in (6), we obtain the following inequality,

$$\begin{aligned} [Q_l(\tau+1)]^2 &\leq [Q_l(\tau)]^2 + \left[ \sum_{n \in \mathcal{N}} \mu_{l,n}^s(\tau) \right]^2 + [A_l(\tau)]^2 \\ &- 2Q_l(\tau) \left[ \sum_{n \in \mathcal{N}} \mu_{l,n}^s(\tau) \right] + 2A_l(\tau)Q_l(\tau). \end{aligned} \quad (18)$$

Summing (18) over all locations  $l \in \mathcal{L}$  and combining  $\sum_{n \in \mathcal{N}} \mu_{l,n}^s(\tau) \leq \mu_{max}$  and  $A_l(\tau) \leq A_{max}$ , we have,

$$\begin{aligned} \frac{1}{2} \sum_{l \in \mathcal{L}} [Q_l(\tau+1)]^2 - Q_l(\tau)^2 &\leq \frac{1}{2} L (A_{max}^2 + \mu_{max}^2) \\ &- \sum_{l \in \mathcal{L}} Q_l(\tau) \left[ \sum_{n \in \mathcal{N}} \mu_{l,n}^s(\tau) - A_l(\tau) \right]. \end{aligned} \quad (19)$$

Taking expectations over  $\mathbf{y}(t)$  and  $\mathbf{x}(t)$  conditioning on  $\mathbf{Q}(t)$ , we obtain the 1-time-slot conditional Lyapunov drift:

$$\Delta_1(\mathbf{Q}(t)) \leq B_1 - \mathbb{E}\left\{ \sum_{l \in \mathcal{L}} Q_l(\tau) \left[ \sum_{n \in \mathcal{N}} \mu_{l,n}^s(\tau) - A_l(\tau) \right] | \mathbf{Q}(t) \right\}. \quad (20)$$

Summing (20) over  $\tau \in [t, t+1, \dots, t+T-1]$ , we obtain:

$$\Delta_T(Q(t)) \leq B_1 T - \mathbb{E} \left\{ \sum_{\tau=t}^{t+T-1} \sum_{l \in \mathcal{L}} Q_l(\tau) \left[ \sum_{n \in \mathcal{N}} \mu_{l,n}^s(\tau) - A_l(\tau) \right] | Q(t) \right\}. \quad (21)$$

Adding the cost term  $V \mathbb{E} \left\{ \sum_{\tau=t}^{t+T-1} C(\tau) \right\}$  to both sides of (21), we prove the theorem. ■

### B. RELAXED LYAPUNOV OPTIMIZATION PROBLEM

The Lyapunov optimization aims to choose control actions to minimize the right-hand side of (17). To achieve this, we need the queue backlogs  $Q_l(\tau)$  in time slots  $\tau = t, \dots, t+T-1$ , which are not available at the beginning of frame  $t$ . Therefore, we approximate the queue backlog at each time slot,  $Q_l(\tau)$ , by the queue backlog at the beginning of the frame,  $Q_l(t)$ . This approximation loosens the upper bound in (17) as shown below. However, we will show our algorithm can still approach the optimal performance with a proven bound in Section IV-G.

*Corollary 1 (Loosening Drift-Plus-Penalty Bound):* Let  $V > 0$  and  $t = kT$  for some nonnegative integer  $k$ . Replacing  $Q(\tau)$ ,  $\tau \in [t, t+T-1]$  with  $Q(t)$ , the drift-plus-penalty satisfies:

$$\Delta_T(t) + V \mathbb{E} \left\{ \sum_{\tau=t}^{t+T-1} C(\tau) \right\} \leq B_2 T + V \mathbb{E} \left\{ \sum_{\tau=t}^{t+T-1} C(\tau) \right\} - \mathbb{E} \left\{ \sum_{\tau=t}^{t+T-1} \sum_{l \in \mathcal{L}} Q_l(t) \left[ \sum_{n \in \mathcal{N}} \mu_{l,n}^s(\tau) - A_l(\tau) \right] | Q(t) \right\}, \quad (22)$$

where  $B_2 = B_1 + \frac{T-1}{2} L \mu_{max} (\mu_{max} - A_{max})$ .

*Proof:* From queuing dynamics (7), for each time slot  $\tau \in [t, t+T-1]$ , the following inequality holds,

$$Q_l(t) - (\tau - t) \mu_{max} \leq Q_l(\tau) \leq Q_l(t) + (\tau - t) A_{max}. \quad (23)$$

Therefore, combining (17), we obtain,

$$\begin{aligned} \Delta_T(t) + V \mathbb{E} \left\{ \sum_{\tau=t}^{t+T-1} C(\tau) \right\} &\leq B_1 T - \mathbb{E} \left\{ \sum_{\tau=t}^{t+T-1} \sum_{l \in \mathcal{L}} [Q_l(t) \right. \\ &\quad \left. - (\tau - t) \mu_{max}] \times \left[ \sum_{n \in \mathcal{N}} \mu_{l,n}^s(\tau) - A_l(\tau) \right] | Q(t) \right\} \\ &\quad + V \mathbb{E} \left\{ \sum_{\tau=t}^{t+T-1} C(\tau) \right\}, \end{aligned} \quad (24)$$

which leads to the following inequality,

$$\begin{aligned} \Delta_T(t) + V \mathbb{E} \left\{ \sum_{\tau=t}^{t+T-1} C(\tau) \right\} &\leq B_1 T - \mathbb{E} \left\{ \sum_{\tau=t}^{t+T-1} \sum_{l \in \mathcal{L}} Q_l(t) \left[ \sum_{n \in \mathcal{N}} \mu_{l,n}^s(\tau) - A_l(\tau) \right] | Q(t) \right\} \\ &\quad + \frac{T(T-1)}{2} L \mu_{max} (\mu_{max} - A_{max}) + V \mathbb{E} \left\{ \sum_{\tau=t}^{t+T-1} C(\tau) \right\}. \end{aligned} \quad (25)$$

By denoting  $B_2 = B_1 + \frac{T-1}{2} L \mu_{max} (\mu_{max} - A_{max})$ , we have (22). ■

The cell activation decisions  $y_n(t)$  and user association decisions  $x_{nk}(t)$  can be determined by minimizing the right-hand side of (22) or equivalently maximizing the following

$$\mathbb{E} \left\{ \sum_{\tau=t}^{t+T-1} \sum_{l \in \mathcal{L}} Q_l(t) \sum_{n \in \mathcal{N}} \mu_{l,n}^s(\tau) | Q(t) \right\} - V \mathbb{E} \left\{ \sum_{\tau=t}^{t+T-1} C(\tau) \right\}, \quad (26)$$

since neither  $\sum_{\tau=t}^{t+T-1} \sum_{l \in \mathcal{L}} Q_l(t) A_l(\tau)$  nor  $B_2 T$  in (22) will be affected by the policy at time slot  $t$ .<sup>6</sup>

### C. ONLINE JOINT SMALL CELL ACTIVATION AND USER ASSOCIATION

Based on the traffic model in section III-C, the average traffic arrival rate of each location is known at the gateway. Given the average traffic arrival rate of locations, (26) is reduced to

$$\begin{aligned} &\mathbb{E} \left\{ \sum_{\tau=t}^{t+T-1} \left[ \sum_{l \in \mathcal{L}} Q_l(t) \sum_{n \in \mathcal{N}} \mu_{l,n}^s(\tau) - V C(\tau) \right] \right\} \\ &= \mathbb{E} \left\{ \sum_{\tau=t}^{t+T-1} \left[ \sum_{l \in \mathcal{L}} Q_l(t) \sum_{n \in \mathcal{N}} \mu_{l,n}^s(\tau) - V \left( \sum_{n \in \mathcal{N}_1} y_n(t) C^W(\tau) \right. \right. \right. \\ &\quad \left. \left. + \sum_{n \in \mathcal{N}_2} y_n(t) C^C(\tau) + C^{co} \right) \right] \right\}, \end{aligned} \quad (27)$$

where  $C^W(\tau) = [P_n^{W,a} - P_n^{W,s}]$ ,  $C^C(\tau) = [P_n^{C,a} - P_n^{C,s}]$  and  $C^{co} = [\sum_{n \in \mathcal{N}_1} P_n^{W,s} + \sum_{n \in \mathcal{N}_2} P_n^{C,s} + P_0^{ov}]$ .

In this case, the original optimization problem can be stated as the joint optimization of small cell activation (finding optimal  $y(t)$ ) at the beginning of each frame and user association (determining optimal  $\mu_{l,n}^s(\tau)$ ) at each time slot. For clarity, the original optimization problem in (13) is further written as

$$\begin{aligned} \text{P2: } \max \quad &\mathbb{E} \left\{ \sum_{\tau=t}^{t+T-1} \left[ \sum_{l \in \mathcal{L}} Q_l(t) \sum_{n \in \mathcal{N}} \mu_{l,n}^s(\tau) - V \tilde{C}(\tau) \right] \right\} \\ \text{s.t. } &(1), (3) \end{aligned} \quad (28)$$

where  $\tilde{C}(\tau) = \sum_{n \in \mathcal{N}_1} y_n(t) C^W(\tau) + \sum_{n \in \mathcal{N}_2} y_n(t) C^C(\tau) + C^{co}$ .

Based on (28), obtaining optimal user association only needs the queue backlog information at the beginning of a frame. This fact together with the assumption that the activation decisions keep unchanged during a frame implies that there is an optimal activation solution to (28) where associations between small cells and locations are constant. However, it is obvious that the optimization problem in (28) is inequivalent to the original optimization problem in (13). In subsection IV-D.2, we analyze the performance gap in detail. While in the following, we will show solutions to the user association and cell activation problems respectively.

<sup>6</sup>Since a frame  $k$  can also be treated as a special time slot  $t$ , we use "time slot" for describing the cell activation and user association decisions unitedly, and when solving them separately in the following subsections, we will differ them with "frame" and "time slot" respectively.

### D. OPTIMAL MATCHING-BASED USER ASSOCIATION

From the above subsections, it is shown that the user association scheme can be developed given the set of active small cell BSs, and this split guarantees the equivalence to the loosened drift-plus-penalty bound maximization problem in (28) rather than the original problem in (13). Specifically, given the set of active small cell BSs  $\mathcal{Y}$ , which consists of active Wi-Fi APs  $n \in \mathcal{Y}_1$  and cellular small cell BSs  $n \in \mathcal{Y}_2$ , the optimization problem in (28) is simplified as:

$$\begin{aligned}
 \text{P3: } \max \quad & \sum_{l \in \mathcal{L}} Q_l(t) [r_{l,0}(\tau) + \sum_{n \in \mathcal{Y}} x_{l,n}(\tau) r_{l,n}(\tau)] \\
 & = \sum_{l \in \mathcal{L}} Q_l(t) r_{l,0}(\tau) + \sum_{l \in \mathcal{L}} \sum_{n \in \mathcal{Y}} Q_l(t) x_{l,n}(\tau) r_{l,n}(\tau) \\
 \text{s.t. } \quad & \sum_{n \in \mathcal{Y}} x_{l,n}(\tau) = 1, \quad \forall l \in \mathcal{L} \\
 & x_{l,n}(\tau) \in \{0, 1\}, \quad \forall l \in \mathcal{L}, \forall n \in \mathcal{Y}
 \end{aligned} \quad (29)$$

which is actually a weighted network throughput maximization problem, and belongs to the class of mixed-integer non-linear programming (MINLP) that is generally NP-hard and has a complexity increasing exponentially with the number of involved small cells and locations.

### 1) USER ASSOCIATION AS A MATCHING GAME

Generally, the distributed solution of an MINLP problem is obtained by either convex optimization after some relaxation and transformation, or game-theoretic methods. However, it is easily found that the formulated problem is difficult to be transformed into a convex problem and the traditional game-theoretic solutions, such as Nash equilibrium, are not suitable. Therefore, we adopt the matching theory [40], [41], which provides distributed solutions with low-complexity to the combinatorial problem that matchups players in two sets depending on their individual information and preference. Thus, the concerned user association problem quite fits into the matching framework and the matching game occurs between small cell BSs in set  $\mathcal{Y}$  and locations in set  $\mathcal{L}$ .

We introduce a two-sided many-to-one matching game where users in each location will be matched to at maximum one small cell BS, while a small cell BS can be assigned to one or more locations. Formally, we have the following definition [42]:

*Definition 1 (Matching Game):* Given two disjoint finite sets of players  $\mathcal{Y}$  and  $\mathcal{L}$ , a matching game  $\rho$  is defined as a function from  $\mathcal{Y} \rightarrow \mathcal{L}$ , where we have 1)  $\forall n \in \mathcal{Y}, \rho(n) \in \mathcal{L}$ , 2)  $\forall l \in \mathcal{L}, \rho(l) \in \mathcal{Y}$ , 3)  $\rho(n) = l$ , if and only if  $n \in \rho(l)$ .

In matching theory, the quota of a player is defined as the maximum number of players that a player can be matched to. Here, the quota of a location is set to be one, while there is no predetermined quota for a small cell BS. In addition, we have  $(l, n) \in \rho$ , if location  $l$  is assigned to small cell BS  $n$  through matching  $\rho$ , and  $(l, n) \notin \rho$  otherwise.

### 2) PREFERENCE ANALYSIS

A preference relation  $\succ$  is defined as a complete, reflexive, and transitive binary relation between players in  $\mathcal{L}$  and  $\mathcal{Y}$ . In this game, each small cell BS in set  $\mathcal{Y}$  aims to serve locations for helping to offload. Hence,  $\max \sum_{l \in \mathcal{L}} \sum_{n \in \mathcal{Y}} U_{l,n}(r_{l,n}, \rho)$ , where  $\rho: \mathcal{L} \rightarrow \mathcal{Y}$  is a matching for assigning users in location  $l \in \mathcal{L}$  to the best small cell  $n \in \mathcal{Y}$ , and  $U_{l,n}(r_{l,n}, \rho) = x_{l,n} r_{l,n} Q_l$  is the utility function for a location  $l \in \mathcal{L}$  serviced by cell  $n \in \mathcal{Y}$ . For  $\rho$  and  $x_{l,n}$ , there is: if  $(n, l) \in \rho$ ,  $x_{l,n} = 1$ , otherwise,  $x_{l,n} = 0$ . Additionally,  $U_n(\rho) = \sum_{l \in \mathcal{L}} x_{l,n} r_{l,n} Q_l$  and  $U_l(\rho) = \sum_{n \in \mathcal{Y}} x_{l,n} r_{l,n} Q_l$  are respectively the utility functions of cell  $n$  and location  $l$ .

Then, for small cell  $n$ , the preference relation  $\succ_n$  over the set of locations  $\mathcal{L}$  is defined as: for any two locations  $l_1, l_2 \in \mathcal{L}^2$ ,  $l_1 \neq l_2$ , and two matchings  $\rho, \rho' \in \mathcal{L} \times \mathcal{Y}$ ,  $l_1 = \rho(n)$ ,  $l_2 = \rho'(n)$ :  $l_1 \succ_n l_2$  if and only if  $U_n(r_{l_1,n}, \rho) > U_n(r_{l_2,n}, \rho')$ ; and similarly, for any location  $l$ , a preference relation  $\succ_l$  is defined over the set of cells  $\mathcal{Y}$  such that, for any two cells  $n_1, n_2 \in \mathcal{Y}^2$ ,  $n_1 \neq n_2$ , and two matchings  $\rho, \rho' \in \mathcal{L} \times \mathcal{Y}$ ,  $n_1 = \rho(l)$ ,  $n_2 = \rho'(l)$ :  $n_1 \succ_l n_2$  if and only if  $U_l(r_{l,n_1}, \rho) > U_l(r_{l,n_2}, \rho')$ . Moreover, by observing (2) and (5), for a location-cell association  $(l, n) \in \rho$ , the downlink long-term rate depends on the other location-cell association  $(i, j) \in \rho$ ,  $(l, n) \neq (i, j)$ . That is, the preferences of all locations and cells are interdependent, i.e., they are influenced by the existing matching. Additionally, externalities are used to describe the dynamic impacts of these external effects on the performance of each user-small cell association, and to study them, matching games with externalities in [42] are suitable.

### 3) DISTRIBUTED SOLUTION

Given the externalities observed in the preferences, once a location-small cell association is established or removed, some locations and small cells may change their preference lists. Thus, a final location-cell association never reaches unless externalities are well handled. On the other hand, since the preference lists change with the reforming of location-cell association, the solutions based on preference lists are unsuitable. Consequently, taking into account the externalities, we have the following definition [43]:

*Definition 2 (Stable Matching):* Given a pair of small cell BSs  $n, m \in \mathcal{Y}$  and locations  $l, v \in \mathcal{L}$ , a matching  $\rho$  with  $(l, n), (v, m) \in \rho$  is stable if no stable swap-matching  $\rho_{n,m}^l = \{\rho \setminus (l, n)\} \cup (l, m)$  exists, such that:  $\forall x \in \{n, m, l, v\}$ ,  $U_x(\rho_{n,m}^l) \geq U_x(\rho)$  and  $\exists x \in \{n, m, l, v\}$ ,  $U_x(\rho_{n,m}^l) > U_x(\rho)$ .

For the studied problem, a matching  $\rho$  with association  $(l, n) \in \rho$  is said to be stable if there does not exist any cell  $m$  or location  $v$ , for which cell  $n$  prefers location  $v$  over  $l$  or any location  $l$  prefers cell  $m$  over  $n$ . Given the externalities in current matching  $\rho$ , to reach the network-wide matching stability, it must be guaranteed that the swaps occur only if they are beneficial for the involved players.

We develop Algorithm 1 to find a stable location-small cell matching for the concerned user association problem.



Initially, each location is associated with the nearest small cell, and a matching  $\rho$  is formed. Then, based on current matching, locations exchange performance metrics with the neighboring small cells. In the second phase, locations and small cells update their utilities and preferences depending on matching  $\rho$ . For a location  $l$ , if the small cell serves it currently (denoted by  $n$ ) is not its most preferred one (denoted by  $m$ ), it sends small cell  $m$  a matching proposal. While for a small cell  $m$ , once a matching proposal is received, it notices the involved small cells and locations to update their utilities and cell  $m$  accepts the proposal only if it is strictly beneficial. Otherwise, cell  $m$  rejects the proposal, and location  $l$  examines small cell  $n$  and the next cell in its preference list. In this way, based on current matching, both locations and small cells update their utilities and preference lists periodically. Eventually, each location is associated with its first preferred small cell.

---

**Algorithm 1** Matching-Based User Association
 

---

**Require:** The utilities and preferences of each set

**Ensure:** Stable matching between locations and small cells

**Initializing:** Each location associates with its nearest small cell

Stage I: Preference Lists Computation

- Locations and small cells exchange their performance metrics information
- Locations (small cells) rank the candidate small cells (locations) based on their preference functions

Stage II: Swap-matching Evaluation

**repeat**

Updating  $U_{nk}(\rho)$  based on current matching  $\rho$

Sorting Locations and small cells by  $\succ_l$  and  $\succ_n$

**if**  $(m, \rho_{n,m}^l) \succ_l(n, \rho)$  **then**

Location  $l$  sends a proposal to small cell  $m$

Involved small cells and locations compute their utility function for the swap matching  $\rho_{n,m}^l$

**if** Swap matching  $\rho_{n,m}^l$  is strictly beneficial **then**

$\mathcal{L}_m \leftarrow \mathcal{L}_m \cup \{l\}, \rho \leftarrow \rho_{n,m}^l$

**else**

Small cell  $m$  refuses the proposal, and location  $l$  examines small cell  $n$  and the next small cell in its preference list

**end if**

**end if**

**until**  $\nexists \rho_{n,m}^l : (m, \rho_{n,m}^l) \succ_l(n, \rho)$  and  $(v, \rho_{n,m}^l) \succ_m(l, \rho)$

Stage III: Association Determination

- Each location associates with its first preferred small cell.
- 

*Remark 2:* From Algorithm 1, it is easily seen that the developed user association scheme depends on the time-varying network characteristics such as cell states (activation or deactivation), queue states (traffic arrivals and departures) and large-scale channel fading.

#### 4) CONVERGENCE ANALYSIS

*Proposition 1 (Convergence of Matching-Based Association Algorithm):* Algorithm 1 reaches a stable matching and converges to a local maximum to the user association problem in (29).

*Proof:* Following the analysis above, we have:

- (1) According to the definition of swap-matching, a swap occurs only if it strictly increases the utilities of the involved players; owing to the small transmission range, locations can only receive effective signals from a few neighboring small cells. Thus, a limited number of swaps may occur.
- (2) Phase II continues until all the possible swaps have been evaluated. Then each location associates with its most preferred small cell, and vice versa. In this case, there exist no swaps among neighboring locations and small cells that can bring further utility improvement.

Hence, when Phase II terminates with no further improvement can be achieved, Algorithm 1 reaches a stable matching and converges to a local maximum of the problem in (29). However, this local maximum may not be that of the original optimization problem in (13). ■

#### E. SMALL CELL ACTIVATION DETERMINATION

According to the above analysis in (IV-C), the activation problem of small cell BSs is given as follows:

$$\begin{aligned}
 \text{P4: } \max \quad & \sum_{\tau=t}^{t+T-1} \left\{ \sum_{l \in \mathcal{L}} \sum_{n \in \mathcal{N}} Q_l(t) y_n(t) x_{l,n}(\tau) r_{l,n}(\tau) \right. \\
 & \left. - \frac{V}{S} \left[ \sum_{n \in \mathcal{N}_1} y_n(t) C^W(\tau) + \sum_{n \in \mathcal{N}_2} y_n(t) C^C(\tau) \right] \right\} \\
 \text{s.t. } & y_n(t) \in \{0, 1\}, \quad \forall n \in \mathcal{N}
 \end{aligned} \quad (30)$$

The assumption that activation decisions do not change during the frame indicates that there is an optimal solution to the above problem in which associations between small cells and locations are constant. Moreover, both  $C^W(\tau)$  and  $C^C(\tau)$  keep unchanged during the whole frame. Then, the above objective function is further written as

$$U(\mathcal{Y}) = \sum_{l \in \mathcal{L}} \sum_{n \in \mathcal{N}} Q_l y_n \bar{x} \bar{r}_{l,n} - \frac{V}{S} \left[ \sum_{n \in \mathcal{N}_1} y_n C^W + \sum_{n \in \mathcal{N}_2} y_n C^C \right], \quad (31)$$

which is a weighted energy cost minimization problem.

$U(\mathcal{Y})$  is the net utility of the system.  $Q_l$  denotes the queue backlog of location  $l$  at the beginning of the current frame. The traffic transferred to small cell  $n$  intending for location  $l$ , i.e.,  $\bar{x} \bar{r}_{l,n}$ , cannot be larger than the traffic it can support, i.e.,  $\bar{x} \bar{r}_{l,n} \leq x_{l,n} r_{l,n}$ . Moreover, the overall traffic allocated to location  $l$  cannot exceed its demand, i.e.,  $r_{l,0} + \sum_{n \in \mathcal{N}} x_{l,n} r_{l,n} \leq Q_l$ . In addition, the problem (30) belongs to the class of maximum facility location problems that are generally NP-hard. Besides, it is noted that  $U(\mathcal{Y})$  is not a submodular

set function, thus the active BS set optimization method based on submodularity theory in [39] cannot be applied.

In this regard, with the intuition of making the best possible decision in each iteration, we present an iterative and heuristic algorithm as shown in Algorithm 2. Specifically, the algorithm starts with an empty activation set  $\mathcal{Y} = \emptyset$ . At each iteration, by solving the user association problem repeatedly with different sets of active small cell BSs, the small cell BS that offers the highest utility is chosen and added to the set of active small cell BSs. This process continues until there exists no small cell BS providing positive utility for the current set of active small cell BSs. Since only one small cell BS is activated in each iteration, the loop is executed at most  $N$  times. Combining this with the low-complexity matching-based user association can give the running time of Algorithm 2.

**Algorithm 2** Heuristic Cell Activation Algorithm

**Require:** The set of all the small cell BSs  $\mathcal{N}$

**Ensure:** The cell activation set  $\mathcal{Y}$

**Begin:**

$\mathcal{Y} \leftarrow \emptyset;$

$continue \leftarrow true;$

**while**  $continue$  **do**

**for**  $\forall n \in \mathcal{N} \setminus \mathcal{Y}$  **do**

Obtain  $U(\mathcal{Y} \cup n)$  where  $\bar{x}r_{l,n}(t) = \min_{\tau \in [t, t+T-1]} \{x_{l,n}(\tau)r_{l,n}(\tau)\}$  according to the user association in Algorithm 1

**end for**

$n^* \leftarrow \arg \max_{n \in \mathcal{N}, n \neq l} U(\mathcal{Y} \cup n) - U(\mathcal{Y});$

$u \leftarrow U(\mathcal{Y} \cup n^*) - U(\mathcal{Y});$

**if**  $u > 0$  **then**

$y_{n^*} = 1;$

$continue \leftarrow true$

**else**

$continue \leftarrow false$

**end if**

**end while**

*Remark 3:* According to the above analysis and Algorithm 2, the cell activation determination considers the time-varying traffic states and large-scale channel fading.

**F. TWO-TIME-SCALE ONLINE JOINT ALGORITHM**

For the formulated energy-aware traffic offloading problem, the cell activation decision  $y(t)$  should be made at the beginning of each large-time-scale (i.e., frame) while user association decision  $x_{l,n}(\tau)$  is made at each small-time-scale (i.e., time slot). The problem is separated into two independent sub-problems as given in (29) and (30) respectively, and their respective solutions are presented in Algorithms 1 and 2. At the end of each time slot, the queue evolution is updated.

To summarize, the solution to the original optimization problem and the implementation of the two-time-scale online joint algorithm are illustrated in Fig. 3.

**Algorithm 3** Two-Time-Scale Online Joint Algorithm

- 1) *Large-time-scale cell activation:* At the beginning of each frame  $t = kT$  ( $k \in \mathbb{R}_+$ ), the state of each small cell BS is determined according to Algorithm 2;
- 2) *Small-time-scale user association:* At each time slot  $\tau \in [t, t + T - 1)$ , the locations decide their association with the active small cells according to Algorithm 1.
- 3) *Queue Update:* Update the queues using (6).

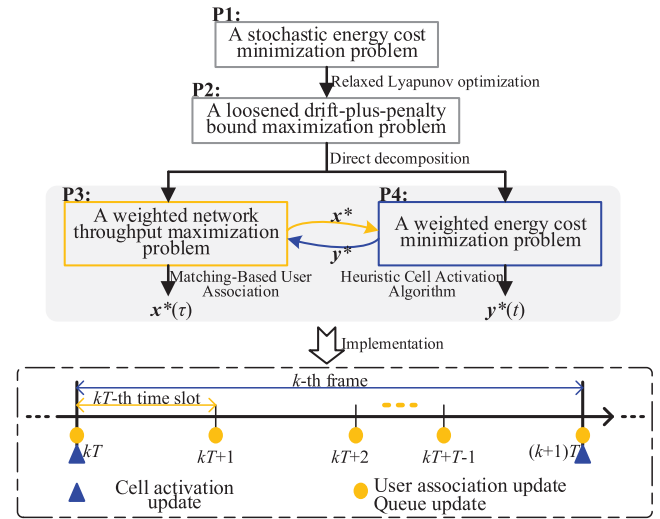


**FIGURE 3.** Solution to the original optimization problem and implementation of the two-time-scale online joint algorithm.

**G. PERFORMANCE ANALYSIS**

We analyze the performance gap of the result achieved by joint algorithm, if the accurate knowledge of  $Q(\tau)$  in the future large-time-scale interval is employed rather than the approximation. We denote by  $C^*$  the theoretical offline optimal value of the objective function of energy cost minimization problem.

*Theorem 2 (Performance Bound):* Assuming that all the queues are empty initially, for a given  $V > 0$ , it has been shown in [38] that any method that maximizes (28) satisfies

$$\limsup_{t \rightarrow \infty} \frac{1}{t} \sum_{\tau=0}^{t-1} C(\tau) \leq C^* + \frac{B_2}{V}. \quad (32)$$

*Proof:* Let  $t = kT$  ( $k \in \mathbb{R}_+$ ) and  $\tau \in [t, t + T - 1]$ . There exists an optimal solution  $C^*$ . Since the proposed online joint algorithm minimizes the right-hand side of (22), plugging the control policy into it, we have:

$$\begin{aligned} \Delta_T(t) + V \mathbb{E} \left\{ \sum_{\tau=t}^{t+T-1} C(\tau) \right\} &\leq B_2 T + V \mathbb{E} \left\{ \sum_{\tau=t}^{t+T-1} C(\tau) \right\} \\ &\leq B_2 T + VTC^*. \end{aligned} \quad (33)$$

By taking expectation of both sides, we obtain:

$$\mathbb{E}\{L(t+T) - L(t)\} + VT \mathbb{E}\{C_{av}(t)\} \leq B_2 T + VTC^*. \quad (34)$$

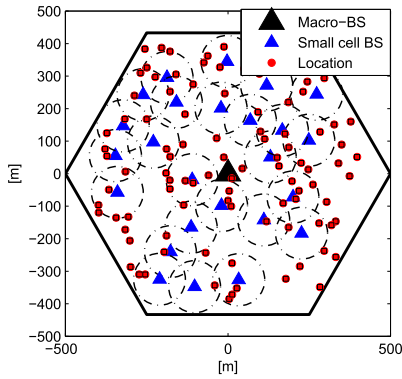


FIGURE 4. A simulation topology.

Summing (34) over  $t = kT, k = 0, 1, 2, \dots, K - 1$ , applying the fact that  $L(t) > 0$ , and dividing both sides by  $VKT$ , we get:

$$\frac{1}{KT} \mathbb{E} \left\{ \sum_{\tau=0}^{KT-1} C_{av}(\tau) \right\} \leq C^* + \frac{B_2}{V}. \quad (35)$$

Taking the limit as  $K \rightarrow \infty$ , we complete the proof. ■

The above theorem indicates that by increasing  $V$  the gap between the optimal energy cost and the achieved one can be made arbitrarily small. Also, it is noted that, as we usually have performance-backlog tradeoff, a larger  $V$  means larger queue size [38].

*Remark 4:* The above Theorem 2 is obtained with the assumption that traffic arrivals are *i.i.d.* over time slots. Referring to [44], it can be extended to the case when traffic arrivals are Markovian. More specifically, in this case, the performance gap can be expressed as  $O(\frac{1}{V})$ .

## V. PERFORMANCE EVALUATION

In this section, firstly, we give the simulation settings. Then, the performance of the proposed matching-based user association algorithm, the heuristic cell activation algorithm, and the joint cell activation and user association algorithm is respectively evaluated.

### A. SIMULATION SETTINGS

We simulate the problem with 1 macrocell network,  $N = 25$  small cell networks and  $L = 120$  locations. The coverage radii of macro-BS and each small cell are set to be 500m and 80m, respectively, and each location has a size of  $15 \times 15 m^2$ . Referring to [28] and [30], we set the time slot length to be 1 second, and the frame length to be 10 seconds, i.e., the frame size  $T = 10$ . The simulation topology is shown in Fig. 4.

#### 1) MACROCELL NETWORK AND CELLULAR SMALL CELL NETWORKS

The average channel power gain between location  $l$  and cellular small cell  $n$  embodies the effects of path-loss and log-normal shadowing. Basic parameters are shown in Table 2. Moreover, for the macro-BS with massive MIMO, we set its power consumption coefficients as  $C_{0,0} = 4, C_{1,0} = 4.8$ ,

TABLE 2. Simulation parameters.

Parameter	Values
Channel bandwidth	10 MHz
Noise power	-169dBm/Hz
Maximum transmission power of macro-BS	46dBm
Maximum transmission power of pico-BS	30dBm
The number of the antennas of macro-BS	100
Static power consumption of pico-BS	13.6W
Coefficient of load-dependent power consumption of pico-BS	4.0
Power consumption of sleep pico-BS	8.6W
Path-loss between macro-BS and location	$128.1 + 37.6 \log_{10} d$ (km)
Path-loss between pico-BS and location	$140.7 + 36.7 \log_{10} d$ (km)
Log-normal shadowing fading	10dB

TABLE 3. Simulation parameters II.

Parameter	Values	Parameter	Values
$E_b$	$22.4 \mu J$	$E_{c,j}(L-n)$	$80L_n + 100j + 80 \mu J$
$T_b$	$28 \mu s$	$T_c$	$100 \mu s$
$E_s$	$100 \mu J$	$P_n^{W,s}$	$5.8W$

$C_{2,0} = 0, C_{3,0} = 2.08 \times 10^{-8}, C_{0,1} = 1, C_{1,1} = 9.5 \times 10^{-8}$  and  $C_{2,1} = 6.25 \times 10^{-8}$ .

#### 2) Wi-Fi NETWORKS

Assuming that all the Wi-Fi APs are randomly distributed spatially and applying the transmission rate function and power consumption function in subsections III-B and III-D, respectively, we give the following simulation parameters for Wi-Fi networks.

#### 3) LOCATIONS

For the traffic arrival  $A_l(t)$  of each location  $l$ , we generate it based on an ergodic Markov chain, and the mean traffic arrival rate per location is set to be 2 Mbps.

## B. NUMERICAL RESULTS

Firstly, with a fixed set of active small cell BSs, we present the convergence and effectiveness of matching-based user association algorithm. Then, the potentials of the heuristic cell activation algorithm are given. Lastly, the performance of joint cell activation and user association algorithm is evaluated.

#### 1) CONVERGENCE AND EFFECTIVENESS OF MATCHING-BASED USER ASSOCIATION ALGORITHM

We focus on the  $1_{st}$  time slot in the  $1_{st}$  frame, i.e.,  $t = 1$  and  $\tau = 1$ , and all the small cells are active. Firstly, Fig. 5 shows the total utility  $U(\tau)$  ( $U(\tau) = \sum_{l \in \mathcal{L}} Q_l(t)[r_{l,0}(\tau) + \sum_{n \in \mathcal{N}} x_{l,n}(\tau)r_{l,n}(\tau)]$ ) versus swaps in a matching-based user association procedure. It is easily observed that the matching game converges in a few number of swaps, and all the swaps increase the total utility. Then, with varying number of locations, Table 4 and Fig. 6 respectively show the average number of swaps to reach convergence and the average percentage of total utility improvement versus the number of small cells and locations. We can easily see that, with the increasing

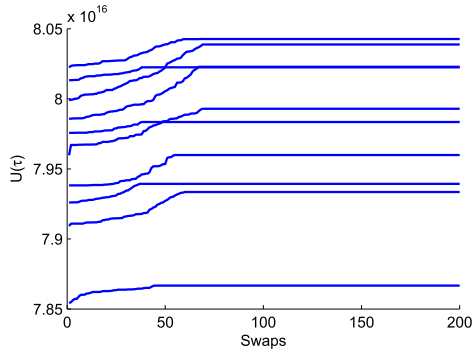


FIGURE 5.  $U(\tau)$  versus swap in 10 matching games.

TABLE 4. Average number of swaps ( $N_s$ ) and average percentage of total utility improvement ( $Per_{impro}$ ) verse number of small cells ( $N$ ).

$N$	10	15	20	25	30	35
$N_s$	16.60	42.63	58.70	59.48	59.85	57.69
$Per_{impro}$	0.07	0.20	0.29	0.32	0.34	0.35

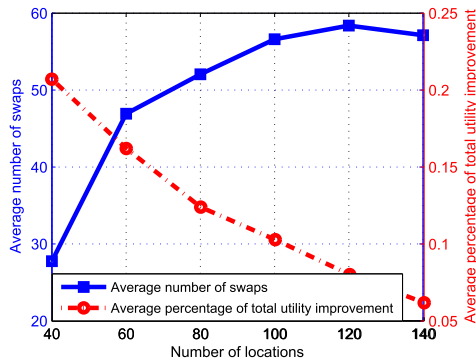


FIGURE 6. Average number of swaps and average percentage of total utility improvement.

number of small cells (locations), the average number of swaps in a matching-based cell selection firstly increases and then decreases since the distribution of small cells and locations gradually evens out, while the average percentage of total utility improvement keeps decreasing slightly.

## 2) POTENTIALS OF HEURISTIC CELL ACTIVATION ALGORITHM

For performance evaluation of the proposed heuristic cell activation algorithm, we still focus on the  $1_{st}$  frame, i.e.,  $t = 1$ , and define  $U(Q) = \sum_{l \in \mathcal{L}} Q_l(t) \sum_{n \in \mathcal{N}} y_n(t) \bar{x} F_{l,n}$  and  $U(C) = \frac{V}{S} [\sum_{n \in \mathcal{N}_1} y_n(t) C^W + \sum_{n \in \mathcal{N}_2} y_n(t) C^C]$ . Firstly, in Fig. 7, we show the evolution of  $U(\mathcal{Y})$ ,  $U(Q)$  and  $U(C)$  in an activation procedure following Algorithm 2 with  $V = 10^{14}$ . Specifically, since each effective step activates a small cell, 17 out of 25 small cells are activated in the considered scenario. Then, the distribution of active and sleep small cells are marked in Fig. 8. Particularly, 13 out of 17 active small cells are pico-BSs, which results from their relative high capacity compared to that of Wi-Fi APs. In addition, the distribution of

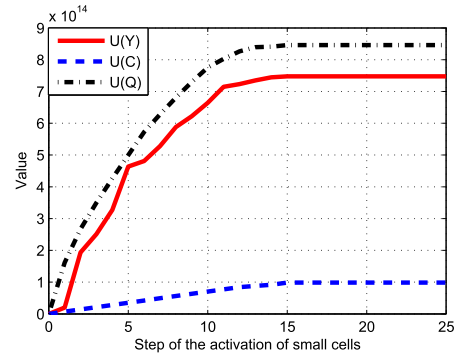


FIGURE 7. Evolution of  $U(\mathcal{Y})$ ,  $U(Q)$  and  $U(C)$ .

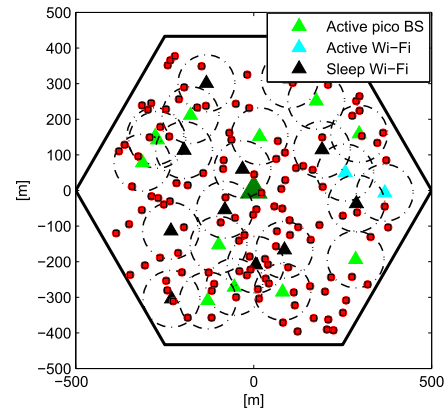


FIGURE 8. Distribution of the active and sleep small cells.

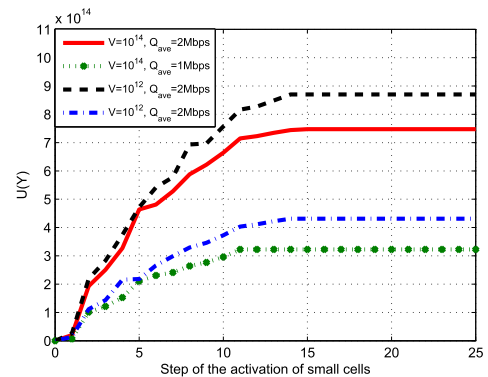


FIGURE 9. Evolution of  $U(\mathcal{Y})$  with different  $V$  and  $Q_{ave}$ .

active small cells facilitates traffic offloading. Further, given fixed small cells and locations, Fig. 9 presents the evolution of  $U(\mathcal{Y})$  with different  $V$  and average queue length  $Q_{ave}$ . It is easily observed that, a larger  $V$  brings smaller  $U(\mathcal{Y})$ , i.e., less weighted energy cost; and a smaller  $Q_{ave}$  needs fewer active small cells and  $U(\mathcal{Y})$  decreases.

## 3) PERFORMANCE EVALUATION OF ONLINE JOINT ALGORITHM

With  $V = 10^{12}$ , Fig. 10 shows the queue dynamics versus time slot in 5 frames. Due to the fact that there are 120 locations,

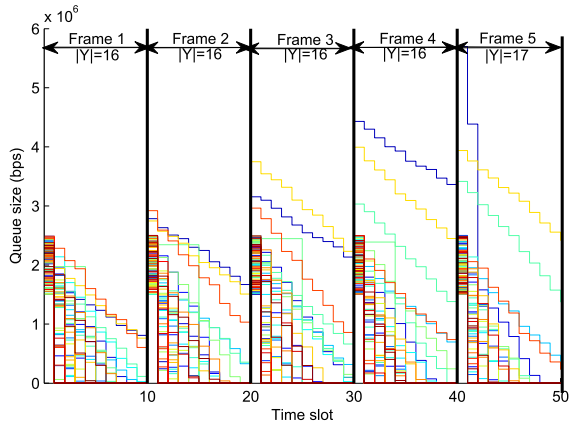


FIGURE 10. Queue dynamics versus time slot in 5 frames ( $V = 10^{12}$ ).

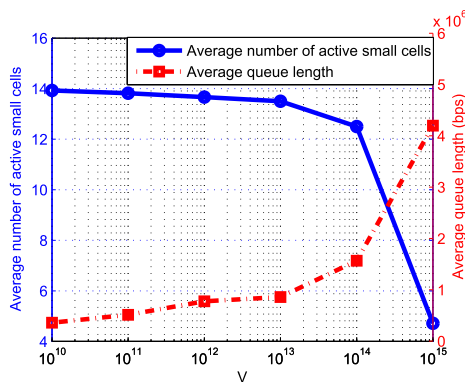


FIGURE 11. Average number of active small cells and average queue length.

i.e., 120 queues, we omit the legend. It is easily observed that, at the beginning of each frame, the cell activation decisions are made based on queue states and delay- or energy cost-aware optimization objective. For example, at frame 5, since the queue backlog seems a little serious, the number of active small cells increases compared with that in other frames. Then in each frame, the small cells help offload through proper location-cell association. Moreover, the matching-based traffic offloading in each time slot of a frame is based on the queue states at the beginning of the frame, and the volume of traffic offloading in the frame varies a little over different time slots due to the large-scale slow-fading of channel power gains.

Then, with different  $V$ s, Fig. 11 presents the average number of active small cells and the average queue length of each location at each time slot in 5 frames. Owing to the time-varying parameters, such as positions, traffic arrivals of locations, and channel fading, we run the joint algorithm for 50 times to get the average values. From Fig. 11, we can easily see that, as  $V$  increases, the average number of active small cells decreases since more emphasis is put on energy cost reduction, which brings more serious queue backlog, i.e., a longer queue of each location at each time slot. While when  $V = 15$ , there are on average less than 5 small cells are activated, and the average queue length increases rapidly.

In a word, when the network optimization targets at reducing energy cost, we should set a reasonably large value to  $V$ . Otherwise,  $V$  should be set to be relatively small if the delay performance is more valued.

## VI. CONCLUSIONS

By considering time-varying and random traffic arrivals, we study the stochastic optimization of joint cell activation and user association for energy cost minimization-oriented traffic offloading via DC. By employing the two-time-scale Lyapunov optimization technique, we transform the formulated problem into a per-frame cell activation problem minimizing the weighted energy cost and a per-time-slot user association problem maximizing the weighted network throughput. Then, without relying on any statistic knowledge of traffic arrivals and channel states, firstly, a matching game with externalities is introduced to distributively solve the user association problem; secondly, a heuristic algorithm is adopted to obtain the optimal set of active small cells; lastly, an online joint cell activation and user association algorithm, which achieves a flexible and efficient tradeoff between energy cost and queuing delay by adjusting a single parameter, is developed. Moreover, we present numerical simulations to demonstrate the convergence and effectiveness of the proposed algorithms.

## REFERENCES

- [1] J. G. Andrews, S. Buzzi, W. Choi, S. V. Hanly, A. Lozano, A. C. K. Soong, and J. C. Zhang, "What will 5G be?" *IEEE J. Sel. Areas Commun.*, vol. 32, no. 6, pp. 1065–1082, Jun. 2014.
- [2] *Introduction of LTE-WLAN Radio Level Integration and Interworking Enhancement Stage-2*, document R2-156737, 3GPP, Nov. 2015.
- [3] 4G Americas, "LTE Aggregation and Unlicensed Spectrum," Nov. 2015. [Online] Available: [http://www.5gamericas.org/files/1214/4648/2397/4G\\_Americas\\_LTE\\_Aggregation\\_Unlicensed\\_Spectrum\\_White\\_Paper\\_-\\_November\\_2015.pdf](http://www.5gamericas.org/files/1214/4648/2397/4G_Americas_LTE_Aggregation_Unlicensed_Spectrum_White_Paper_-_November_2015.pdf)
- [4] *Evolved Universal Terrestrial Radio Access Network (EUTRAN); X2 Interface User Plane Protocol*, document TS 36.425, 3GPP, Mar. 2015.
- [5] C. Rosa, K. Pedersen, H. Wang, P.-H. Michaelsen, S. Barbera, E. Malkamaki, T. Henttonen, and B. Sebire, "Dual connectivity for LTE small cell evolution: Functionality and performance aspects," *IEEE Commun. Mag.*, vol. 54, no. 6, pp. 137–143, Jun. 2016.
- [6] X. Huang, S. Tang, Q. Zheng, D. Zhang, and Q. Chen, "Dynamic femtocell gNB on/off strategies and seamless dual connectivity in 5G heterogeneous cellular networks," *IEEE Access*, vol. 6, pp. 21359–21368, May 2018.
- [7] M. Polese, M. Giordani, M. Mezzavilla, S. Rangan, and M. Zorzi, "Improved handover through dual connectivity in 5G mmWave mobile networks," *IEEE J. Sel. Areas Commun.*, vol. 35, no. 9, pp. 2069–2084, Sep. 2017.
- [8] Qualcomm Technologies, Inc. "Delivering on the LTE advanced promise," Mar. 2016. [Online] Available: <https://www.qualcomm.com/media/documents/files/delivering-on-the-lte-advanced-promise.pdf>
- [9] D. Astely, E. Dahlman, G. Fodor, S. Parkvall, and J. Sachs, "LTE release 12 and beyond [accepted from open call]," *IEEE Commun. Mag.*, vol. 51, no. 7, pp. 154–160, Jul. 2013.
- [10] 5G Americas, "Wireless technology evolution towards 5G—3GPP release 13 to release 15 and beyond," Feb. 2017. [Online]. Available: [http://www.4gamericas.com/files/6814/8718/2308/3GPP\\_Rel\\_13\\_15\\_Final\\_to\\_Upload\\_2.14.17\\_AB.pdf](http://www.4gamericas.com/files/6814/8718/2308/3GPP_Rel_13_15_Final_to_Upload_2.14.17_AB.pdf)
- [11] Y. Wu, L. P. Qian, J. Zheng, H. Zhou, and X. S. Shen, "Green-oriented traffic offloading through dual connectivity in future heterogeneous small cell networks," *IEEE Commun. Mag.*, vol. 56, no. 5, pp. 140–147, May 2018.
- [12] Q. Han, B. Yang, C. Chen, and X. Guan, "Matching-based cell selection for proportional fair throughput boosting via dual-connectivity," in *Proc. IEEE WCNC*, Mar. 2017, pp. 1–6.
- [13] E. Oh, B. Krishnamachari, X. Liu, and Z. Niu, "Toward dynamic energy-efficient operation of cellular network infrastructure," *IEEE Commun. Mag.*, vol. 49, no. 6, pp. 56–61, Jun. 2011.

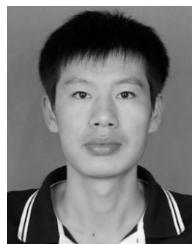
- [14] J. B. Rao and A. O. Fapojuwo, "A survey of energy efficient resource management techniques for multicell cellular networks," *IEEE Commun. Surveys Tuts.*, vol. 16, no. 1, pp. 154–180, 1st Quart., 2014.
- [15] M. Ismail, W. Zhuang, E. Serpedin, and K. Qaraqe, "A survey on green mobile networking: From the perspectives of network operators and mobile users," *IEEE Commun. Surveys Tuts.*, vol. 17, no. 3, pp. 1535–1556, 3rd Quart., 2015.
- [16] K. Kanwal, G. A. Safdar, M. Ur-Rehman, and X. Yang, "Energy management in LTE networks," *IEEE Access*, vol. 5, pp. 4264–4284, 2017.
- [17] M. A. Marsan and M. Meo, "Green wireless networking: Three questions," in *Proc. IFIP Med-Hoc-Net*, Sicily, Italy, Jun. 2011, pp. 41–44.
- [18] Y. Cui, V. K. N. Lau, R. Wang, H. Huang, and S. Zhang, "A survey on delay-aware resource control for wireless systems—Large deviation theory, stochastic Lyapunov drift, and distributed stochastic learning," *IEEE Trans. Inf. Theory*, vol. 58, no. 3, pp. 1677–1701, Mar. 2012.
- [19] M. A. Lena, E. Pardo, O. Galinina, S. Andreev, and M. Dohler, "Flexible dual-connectivity spectrum aggregation for decoupled uplink and downlink access in 5G heterogeneous systems," *IEEE J. Sel. Areas Commun.*, vol. 34, no. 11, pp. 2851–2865, Nov. 2016.
- [20] M. A. Molfafet, N. Mokari, R. Joda, M. R. Sabagh, and M. Zorzi, "Joint access and fronthaul resource allocation in dual connectivity and CoMP based networks," in *Proc. IEEE ICC*, May 2018, pp. 1–6.
- [21] S. Singh, M. Geraseminko, S.-P. Yeh, N. Himayat, and S. Talwar, "Proportional fair traffic splitting and aggregation in heterogeneous wireless networks," *IEEE Commun. Lett.*, vol. 20, no. 5, pp. 1010–1013, Mar. 2016.
- [22] Y. Wu, Y. He, L. Qian, and X. S. Shen, "Traffic scheduling and power allocations for mobile data offloading via dual-connectivity," in *Proc. IEEE ICC*, May 2016, pp. 1–6.
- [23] Y. Wu, Y. He, L. Qian, J. Huang, and X. S. Shen, "Optimal resource allocations for mobile data offloading via dual-connectivity," *IEEE Trans. Mobile Comput.*, vol. 17, no. 10, pp. 2349–2365, Oct. 2018.
- [24] W. Lee, J. Koo, Y. Park, and S. Choi, "Transfer time, energy, and quota-aware multi-RAT operation scheme in smartphone," *IEEE Trans. Veh. Technol.*, vol. 65, no. 1, pp. 307–317, Jan. 2016.
- [25] A. Ekti, X. Wang, M. Ismail, E. Serpedin, and K. A. Qaraqe, "Joint user association and data rate allocation in heterogeneous wireless networks," *IEEE Trans. Veh. Technol.*, vol. 65, no. 9, pp. 7403–7414, Sep. 2016.
- [26] M. Gapeyenko, V. Petrov, D. Moltchanov, M. R. Akdeniz, S. Andreev, N. Himayat, and Y. Koucheryavy, "On the degree of multi-connectivity in 5G millimeter-wave cellular urban deployments," *IEEE Trans. Veh. Technol.*, vol. 68, no. 2, pp. 1973–1978, Feb. 2019.
- [27] K. Son, H. Kim, Y. Yi, and B. Krishnamachari, "Base station operation and user association mechanisms for energy-delay tradeoffs in green cellular networks," *IEEE J. Sel. Areas Commun.*, vol. 29, no. 8, pp. 1525–1536, Sep. 2011.
- [28] A. Abbasi and M. Ghaderi, "Energy cost reduction in cellular networks through dynamic base station activation," in *Proc. 11th Annu. IEEE SECON*, Jun. 2014, pp. 363–371.
- [29] J. Li, J. Wu, M. Peng, and P. Zhang, "Queue-aware energy-efficient joint remote radio head activation and beamforming in cloud radio access networks," *IEEE Trans. Wireless Commun.*, vol. 15, no. 6, pp. 3880–3894, Jun. 2016.
- [30] H. Yu, M. H. Cheung, L. Huang, and J. Huang, "Power-delay tradeoff with predictive scheduling in integrated cellular and Wi-Fi networks," *IEEE J. Sel. Areas Commun.*, vol. 34, no. 4, pp. 735–742, Apr. 2016.
- [31] E. Aryafar, A. Keshavarz-Haddad, M. Wang, and M. Chiang, "RAT selection games in HetNets," in *Proc. IEEE INFOCOM*, Apr. 2013, pp. 998–1006.
- [32] G. Bianchi, "Performance analysis of the IEEE 802.11 distributed coordination function," *IEEE J. Sel. Areas Commun.*, vol. 18, no. 3, pp. 535–547, Mar. 2000.
- [33] D. Bethanabhotla, O. Y. Bursalioğlu, H. C. Papadopoulos, and G. Caire, "Optimal user-cell association for massive MIMO wireless networks," *IEEE Trans. Wireless Commun.*, vol. 15, no. 3, pp. 1835–1850, Mar. 2016.
- [34] Q. Han, B. Yang, G. Miao, C. Chen, X. Wang, and X. Guan, "Backhaul-aware user association and resource allocation for energy-constrained HetNets," *IEEE Trans. Veh. Technol.*, vol. 66, no. 1, pp. 580–593, Jan. 2017.
- [35] B. H. Jung, H. Jin, and D. K. Sung, "Adaptive transmission power control and rate selection scheme for maximizing energy efficiency of IEEE 802.11 stations," in *Proc. IEEE PIMRC*, Sep. 2012, pp. 266–271.
- [36] G. Auer, V. Giannini, C. Desset, I. Godor, P. Skillermark, M. Olsson, M. A. Imran, D. Sabella, M. Gonzalez, O. Blume, and A. Fehske, "How much energy is needed to run a wireless network?" *IEEE Trans. Wireless Commun.*, vol. 18, no. 5, pp. 40–49, Oct. 2011.
- [37] E. Björnson, L. Sanguinetti, J. Hoydis, and M. Debbah, "Designing multiuser MIMO for energy efficiency: When is massive MIMO the answer?" in *Proc. IEEE WCNC*, Apr. 2014, pp. 1–6.
- [38] M. J. Neely, "Stochastic network optimization with application to communication and queueing systems," *Synth. Lectures Commun. Netw.*, vol. 3, no. 1, pp. 1–211, 2010.
- [39] Y. Yang, L. Chen, W. Dong, and W. Wang, "Active base station set optimization for minimal energy consumption in green cellular networks," *IEEE Trans. Veh. Technol.*, vol. 66, no. 11, pp. 5340–5349, Nov. 2015.
- [40] Y. Gu, W. Saad, M. Bennis, M. Debbah, and Z. Han, "Matching theory for future wireless networks: Fundamentals and applications," *IEEE Commun. Mag.*, vol. 53, no. 5, pp. 52–59, May 2015.
- [41] H. Shao, H. Zhao, Y. Sun, J. Zhang, and Y. Xu, "QoE-aware downlink user-cell association in small cell networks: A transfer-matching game theoretic solution with peer effects," *IEEE Access*, vol. 4, pp. 10029–10041, Nov. 2016.
- [42] A. Roth and M. A. O. Sotomayor, *Two-Sided Matching: A Study in Game-Theoretic Modeling and Analysis*. New York, NY, USA: Cambridge Univ. Press, 1992.
- [43] F. Pantisano, M. Bennis, W. Saad, S. Valentin, and M. Debbah, "Matching with externalities for context-aware user-cell association in small cell networks," in *Proc. IEEE GLOBECOM*, Dec. 2013, pp. 4483–4488.
- [44] Y. Yao, L. Huang, A. B. Sharma, L. Golubchik, and M. J. Neely, "Power cost reduction in distributed data centers: A two-time-scale approach for delay tolerant workloads," *IEEE Trans. Parallel Distrib. Syst.*, vol. 25, no. 1, pp. 200–211, Jan. 2014.



QIAONI HAN received the B.S. and M.S. degrees from the Institute of Electrical Engineering, Yanshan University, China, in 2010 and 2013, respectively, and the Ph.D. degree from the School of Electronic and Electric Engineering, Shanghai Jiao Tong University, Shanghai, China, in 2017. She was an Assistant Professor with Qingdao University and selected for the Young Talents Program. She joined Tianjin University in 2019. Her research interests include game theoretical analysis, and resource allocation optimization of wireless networks and energy networks.



BO YANG (SM'16) received the Ph.D. degree in electrical engineering from the City University of Hong Kong, Hong Kong, in 2009. He was a Postdoctoral Researcher with the Royal Institute of Technology, Stockholm, Sweden, from 2009 to 2010, and a Visiting Scholar with the Polytechnic Institute of New York University, in 2007. He joined Shanghai Jiao Tong University, in 2010, where he is currently a Full Professor. He has published over 110 papers. His research interests include game theoretical analysis, and optimization of energy networks and wireless networks. He has been the Principal Investigator for several research projects, including the NSFC Key Project. He was a recipient of the National Youth Support Talent Program 2018, the Shanghai Technological Invention Award 2017, the Ministry of Education Natural Science Award 2016, the Shanghai Rising-Star Program 2015, and the SMC-Excellent Professorship in Shanghai Jiao Tong University. He is on the Editorial Board of *Digital Signal Processing* (Elsevier) and serves on the TPC of several international conferences.



XIAOCHENG WANG received the M.S. degree from the Institute of Electrical Engineering, Yanshan University, China, in 2013, and the Ph.D. degree from the School of Electronic and Electric Engineering, Shanghai Jiao Tong University, Shanghai, China, in 2019. His research interests include game-based spectrum sharing in cognitive radio networks and resource allocation optimizing in green wireless networks.